Eur Radiol (2009) 19: 2679–2688
DOI 10.1007/s00330-009-1473-8

Reto Sutter
Christina Heilmaier
Amelie M. Lutz
Dominik Weishaupt
Burkhardt Seifert
Jürgen K. Willmann

MR angiography with parallel acquisition for assessment of the visceral arteries: comparison with conventional MR angiography and 64-detector-row computed tomography

Received: 26 January 2009
Revised: 1 April 2009
Accepted: 24 April 2009
Published online: 13 June 2009

R. Sutter · A. M. Lutz · D. Weishaupt · J. K. Willmann
Institute of Diagnostic Radiology,
University Hospital Zurich,
Zurich, Switzerland

R. Sutter
Department of Radiology,
Cantonal Hospital Winterthur,
Winterthur, Switzerland

C. Heilmaier
Department of Diagnostic and Interventional Radiology and Neuroradiology,
University Hospital Essen,
Essen, Germany

A. M. Lutz · J. K. Willmann (✉)
Department of Radiology,
Stanford University School of Medicine,
300 Pasteur Dr., Room H1307,
Stanford, CA, 94305-5621, USA
e-mail: willmann@stanford.edu
Tel.: +1-650-7235424
Fax: +1-650-7231909

D. Weishaupt
Department of Radiology,
Hospital Triemli,
Zurich, Switzerland

B. Seifert
Biostatistics Unit,
Institute of Social and Preventive Medicine, University of Zurich,
Zurich, Switzerland

Abstract The purpose of the study was to retrospectively compare three-dimensional gadolinium-enhanced magnetic resonance angiography (conventional MRA) with MRA accelerated by a parallel acquisition technique (fast MRA) for the assessment of visceral arteries, using 64-detector-row computed tomography angiography (MDCTA) as the reference standard. Eighteen patients underwent fast MRA (imaging time 17 s), conventional MRA (29 s) and MDCTA of the abdomen and pelvis. Two independent readers assessed subjective image quality and the presence of arterial stenosis. Data were analysed on per-patient and per-segment bases. Fast MRA yielded better subjective image quality in all segments compared with conventional MRA (P=0.012 for reader 1, P=0.055 for reader 2) because of fewer motion-induced artefacts. Sensitivity and specificity of fast MRA for the detection of arterial stenosis were 100% for both readers. Sensitivity of conventional MRA was 89% for both readers, and specificity was 100% (reader 1) and 99% (reader 2). Differences in sensitivity between the two types of MRA were not significant for either reader. Interobserver agreement for the detection of arterial stenosis was excellent for fast (κ=1.00) and good for conventional MRA (κ=0.76). Thus, subjective image quality of visceral arteries remains good on fast MRA compared with conventional MRA, and the two techniques do not differ substantially in the grading of arterial stenosis, despite the markedly reduced acquisition time of fast MRA.

Keywords Three-dimensional magnetic resonance angiography · Parallel imaging · Arterial stenosis · Visceral arteries

Introduction

Because of its high spatial resolution and wide clinical availability, diagnostic angiography of visceral arteries is usually performed by multi-detector-row computed tomography angiography (MDCTA) [1–3]. While the first reports on contrast-enhanced three-dimensional (3D) magnetic resonance angiography (MRA) of visceral arteries were published in the late 1990s [4–6], widespread clinical use of conventional 3D MRA has been hampered by several disadvantages compared with MDCTA such as lower spatial resolution and longer breath-hold times with consequent impaired image quality [7–9]. In particular, image quality in patients with compromised respiratory

function or patients unable to remain still during data acquisition tends to be impaired using conventional MRA.

The introduction of parallel imaging techniques such as the simultaneous acquisition of spatial harmonics [10] or sensitivity encoding [11] have re-strengthened the role of MRA in assessing the abdominal vasculature. Recent reports have shown a considerably reduced acquisition time for MRA studies of the abdomen with substantially improved image quality of hepatic vessels on fast MRA using either parallel gradient echo sequences [12–14] or generalised autocalibrating partially parallel acquisition sequences [15, 16]. In these studies, fast MRA was tailored to include the liver with a maximum interpolated voxel length on the z-axis of 2.0–2.5 mm [12–14] and 1.5–1.6 mm [15, 16].

Recently, a sensitivity-encoding-based fast MRA technique was introduced that allows assessment of an extended anatomical field-of-view covering the entire abdomen and pelvis at a substantially improved interpolated z-axis resolution of 0.9 mm. Because of markedly reduced acquisition times of 17 s on average with consequently minimised motion-induced artefacts, the image quality of the aorto-iliac and renal arteries using this fast MRA technique has substantially improved compared with conventional MRA, particularly in the assessment of small arteries such as the distal segments of the renal arteries [17]. In the current study, we hypothesised that the image quality of the visceral arteries might also be improved on fast MRA compared with conventional MRA because of reduced motion-related artefacts at faster acquisition times.

Thus, the purpose of our study was to retrospectively compare three-dimensional gadolinium-enhanced magnetic resonance angiography (conventional MRA) with MRA accelerated by a parallel acquisition technique (fast MRA) in the same patient for the assessment of visceral arteries, using 64-detector-row computed tomography angiography (MDCTA) as a reference standard.

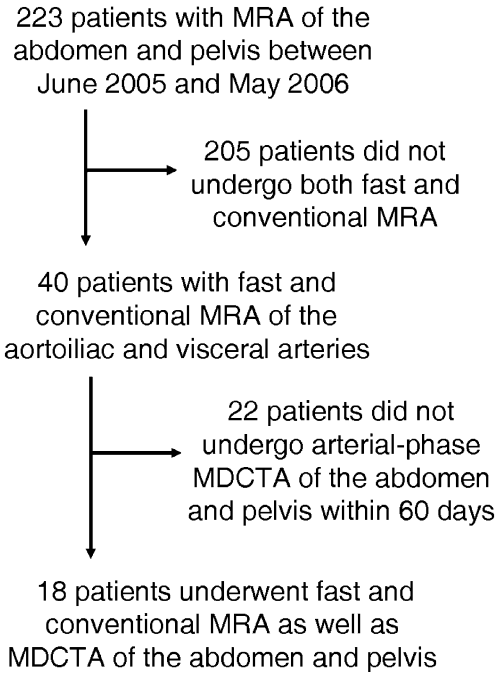

Fig. 1 Patient selection for retrospective study. All patients underwent conventional and fast MRA of the abdomen and pelvis as well as arterial phase 64-detector-row CT angiography (MDCTA) of the abdomen and pelvis within a 60-day period

Materials and methods

Patients

This retrospective study was approved by the hospital's institutional review board, and written informed consent was waived. We cross-referenced our institutional medical database to identify all patients who underwent both fast MRA and conventional MRA imaging of the aorto-iliac and visceral arteries as well as 64-detector-row CT angiography (MDCTA) of the abdomen and pelvis within a 60-day time interval (mean 23 days, range 5–60 days) during the period between June 2005 and May 2006 (Fig. 1). A total of 18 patients were included in the study. In one of the 18 patients (6%), a minor contrast material reaction (rash) was documented after MDCTA. No contrast material reaction was noted after MR imaging. MDCTA was performed before MR in 15/18 patients (84%). No therapeutic vascular intervention was performed between MDCTA and MRA imaging or between the two types of MRA. The study group consisted of 15 men aged 27–77 years (mean 61 years) and 3 women aged 26–73 years (mean 53 years). There was no statistically significant difference between men and women with regard to age (P=0.53). None of the patients presented with symptoms of acute or chronic mesenteric ischaemia.

Magnetic resonance angiography techniques

In all patients, fast MRA and conventional MRA acquisitions were performed on two different days. MRA was acquired with a 1.5-T MR system (Signa Excite HD, GE Healthcare, Waukesha, WI) with a maximum gradient amplitude of 33 mT/m and a slew rate of 120 mT m^{-1} ms^{-1}. All patients were positioned supine and feet-first on the scan table. An anteroposterior eight-element phased-array surface coil was placed around the patient for signal reception, covering the entire abdominal aorta and its visceral branches along with the iliac arteries. Four coil elements were placed above and four elements beneath the patient.

In all MR sessions, the transit time of a 1-mL test bolus of gadobutrol (Gadovist, Bayer Schering, Berlin, Germany) between the injection site (antecubital fossa) and the

abdominal aorta was determined with a multiphase sagittal, single-section gradient-recalled echo sequence (TR/TE 5/1 ms, flip angle 60°). The test bolus was administered through a 20-gauge needle at a flow rate of 2 mL/s by an automated injector (MR Spectris; Medrad, Pittsburgh, PA) and was followed by a 25-mL normal saline flush administered at the same flow rate. Mean transit time was 24 s for both conventional and fast MRA (range 20–27 s). During test bolus administration, the delay between injection and the first major peak of enhancement was measured in the abdominal aorta. The same delay was used between the injection and the initiation of imaging for both types of MRA. Determination of the transit time was performed in end-inspiration breath-holding. In all patients transit times were identical to within 1 s in the two MRA sessions.

In both MRA protocols, a 3D fast spoiled gradient-echo sequence acquired 48 oblique coronal sections with a slice thickness of 1.6 mm in all patients [18–20]. The conventional MRA protocol used the following parameters: TR/TE 3.5/0.9 ms, flip angle 25°, receiver bandwidth ±62.5 kHz, matrix 256×192, field-of-view 44×35.2 cm. In the fast MRA protocol, an increased field-of-view of 48.0×38.4 cm with a matrix of 280×236 was used to consistently avoid parallel imaging artefacts [21] (see below). The associated increase in matrix size resulted in increased TR/TE times of 4.2 and 1.3 ms respectively, despite increased receiver bandwidth of ±83.3 kHz. Both MRA data sets were interpolated to a larger matrix size and an interpolated voxel size of 0.9×0.9×0.8 mm during reconstruction, and both MRA acquisitions featured a centric elliptical phase-encode ordering. Gadobutrol was administered at a dose of 0.1 mmol/kg of body weight at a flow rate of 2 mL/s followed by a 25-mL normal saline flush at the same flow rate. The range of the total volume of gadobutrol for both MRA sessions was 13–24 mL, according to patient weight. MR data acquisition was obtained in an end-inspiration breath-hold.

For fast MRA, a commercial implementation (ASSET: array spatial sensitivity encoding technique; GE Healthcare, Milwaukee, WI) of the sensitivity encoding (SENSE) technique [11] was used. This technique reconstructs the full field-of-view by evaluation of the inter-coil variation of the superimposed "true" and aliased signal intensities in the under-sampled data set. The reconstruction algorithm cannot consistently correct artefacts caused by a signal from outside the phase-encoding field-of-view that is aliased more than once in the undersampled data set. In contrast to conventional acquisitions with the aliased signal intensity appearing along the image edges, the corresponding artefacts in parallel acquisitions often appear in the image centre [21]. Thus, the minimum reconstructed field-of-view in parallel acquisitions is moderately large compared with the minimum field-of-view in conventional acquisitions. The acceleration factor was set to 2 for fast MRA. The mean acquisition time of fast MRA was 17 s compared with 29 s for conventional MRA.

64-Detector-row computed tomography angiography

In all patients, multi-detector-row CT images of the abdomen were obtained with a 64-detector-row CT system (Sensation 64, Siemens, Forchheim, Germany). All patients underwent MDCTA of the abdomen and pelvis acquired during the arterial phase of the contrast enhancement.

Before imaging, a 20-gauge catheter was placed in an antecubital vein and attached to an automated injector (Ulrich Medical, Ulm-Jungingen, Germany). A bolus-tracking technique (CARE-Bolus, Sensation Navigator, Siemens, Forchheim, Germany) was used to define the optimal time delay after administration of the contrast medium in order to achieve optimal intraluminal contrast enhancement during the arterial phase of the contrast medium. This technique encompassed a single, non-enhanced, low-dose CT acquisition (10 mA) at the level of the celiac trunk, where a region of interest (ROI) with an area of 15–20 mm^2 was set in the aorta by a technologist. Subsequently, 120 mL of non-ionic, iodinated contrast medium (Iodixanol, Visipaque, Amersham Health, Buckinghamshire, UK; 270 mg iodine per mL) was administered at a flow rate of 4 mL/s, followed by a 20-mL flush of saline injected at the same flow rate. Ten seconds after the start of the contrast medium administration, repetitive low-dose monitoring CT images (120 kV, 10 mA, 0.5 s) were performed every 1.5 s until the preset contrast enhancement level of 120 HU was reached within the ROI. This resulted in the automatic initiation of MDCTA. The CT parameters for this main CTA acquisition were a section thickness of 0.6 mm, a table-feed of 46 mm per rotation, and a 0.5 s gantry rotation time (pitch 1.2). The X-ray tube voltage setting was 120 kV at a mean tube current of 150 mA. Transverse section reconstructions were performed with a nominal slice thickness of 1.0 mm at an interval of 0.4 mm for both phases of contrast medium [22]. The reconstruction field-of-view was set according to the patient's size and ranged between 25 and 45 cm at a matrix size of 512×512.

MR image analysis—quantitative

Images were quantitatively and qualitatively analysed on a dedicated interactive workstation (Advantage Windows Workstation 4.2, GE Healthcare, Buc, France). Signal-to-noise ratios (SNRs) and contrast-to-noise ratios (CNRs) were measured for fast MRA and conventional MRA by one author who was blinded to all patient data. Quantitative image analysis was carried out randomly with regard to patient order and type of MRA. Measurements were performed in eight anatomical segments: the supra- and infrarenal abdominal aorta, the proximal segment of the celiac artery, the common hepatic artery, the splenic artery, the left gastric artery, as well as in the superior and inferior mesenteric arteries. Measurements were performed in a total of 141/144 arterial segments in fast MRA (98%; all

arterial segments with moderate or better visibility as rated by both readers, see below) and in 138/144 arterial segments in conventional MRA (96%). Reader-defined ROIs were placed in the middle of the respective artery, in the adjacent fat, and in an image region in the air adjacent to the body within the coil. ROIs were set to encompass as much as possible of the different arteries under consideration (mean 20 mm^2; range 5–180 mm^2). SNR and CNR measurements were calculated as follows: SNR = mean signal intensity in the artery/standard deviation of the magnitude background signal outside the body within the coil (air); CNR = (mean signal intensity in the artery − mean signal intensity in the adjacent fat)/standard deviation of the magnitude background signal outside the body within the coil (air). SNR and CNR are generally lower when using parallel imaging compared with conventional MRA; furthermore, the signal intensity may vary over the image [23]. Nevertheless, SNR and CNR were used in this study as valid imaging parameters when comparing conventional with parallel MRA [23, 24].

MR image analysis—qualitative

For qualitative analysis, the arterial vascular system was also divided into eight anatomical segments (total of 141 segments). Two readers, who were blinded to the name of the patient, the clinical data and the type of MRA, independently assessed subjective image quality of all arterial segments on both types of MRA in random order. The readers were allowed to individually adjust window centres and level settings of the MR data sets for image analysis on the workstation, and a ciné mode was available for rapid interactive interpretation. In addition, both readers were allowed to use maximum intensity projections of the MR data sets in different planes if considered useful. The image quality of each vessel was graded on a five-point Likert scale: 1, not visible (no diagnostic information can be obtained from the images); 2, poor visibility (image quality of the vessel is degraded because of low signal intensity *and* motion-induced blurring artefacts); 3, moderate visibility (image quality of the vessel is degraded because of low signal intensity *or* motion-induced blurring artefacts); 4, good visibility (high signal intensity and slight motion-induced blurring artefacts); 5, excellent visibility (high signal intensity, no motion-induced blurring artefacts). The presence of arterial stenosis was ranked independently by both readers as follows: grade 1, normal vessel or vessel irregularities (< 10% luminal narrowing); grade 2, mild arterial stenosis (< 50% luminal narrowing); grade 3, severe arterial stenosis (50-99% luminal narrowing); grade 4, occlusion. For the purposes of the study, grades 3 and 4 (50-100% luminal narrowing) were defined as haemodynamically significant arterial stenosis. When two or more stenotic lesions were detected in the same arterial segment, the most severe change was used for grading and analysis.

MDCTA image analysis

All MDCTA images were evaluated by a consensus panel consisting of two additional readers on the basis of the transverse MDCT source data available on the interactive workstation (Advantage Windows Workstation 4.2, GE Healthcare, Buc, France). The readers were allowed to adjust window centres and level settings to their own preference and to make use of transverse or oblique maximum intensity projections of the MDCTA data sets, if considered useful. Both readers were blinded to all clinical data and MRA results. The consensus diagnosis of the MDCTA data sets was defined as the standard of reference in this study. In two patients with two stenotic segments, plaque calcification was seen on MDCT angiograms.

Table 1 Measurements of signal-to-noise and contrast-to-noise ratios for abdominal aorta and visceral arteries on conventional and fast magnetic resonance angiography images in 18 patients

	Signal-to-noise ratio			Contrast-to-noise ratio		
	Conventional MRA	Fast MRA	*P* value	Conventional MRA	Fast MRA	*P* value
Suprarenal aorta	61.9±10.7	26.0±4.5	< 0.001	48.6±9.6	21.7±3.6	< 0.001
Infrarenal aorta	59.6±9.5	34.7±5.9	< 0.001	44.8±8.2	28.8±5.2	< 0.001
Celiac trunk	58.6±9.1	26.8±3.6	< 0.001	44.9±10.1	21.8±2.7	< 0.001
Left gastric artery	37.6±8.5	18.2±3.5	< 0.001	23.4±5.2	13.2±2.7	< 0.001
Splenic artery	51.9±9.7	27.3±5.7	< 0.001	37.6±7.6	21.9±4.5	< 0.001
Common hepatic artery	55.9±14.1	24.1±3.5	< 0.001	42.3±9.3	18.8±2.4	< 0.001
Superior mesenteric artery	59.0±7.5	28.9±3.7	< 0.001	44.5±6.8	24.1±3.0	< 0.001
Inferior mesenteric artery	39.3±17.8	17.7±4.1	0.001	25.7±16.2	14.2±3.9	0.001

Numbers are means ± standard deviations. *P* values < 0.0063 are considered statistically significant (after Bonferroni correction)
MRA Magnetic resonance angiography

Statistical analysis

SNR and CNR are presented as mean ± standard deviation. The Wilcoxon signed rank test was used for assessment of differences between both types of MRA with regard to SNR and CNR. After Bonferroni correction to adjust for multiple comparisons in eight arterial segments, a comparison-wise P value of less than 0.0063 was considered to indicate a statistically significant difference. Age differences between women and men were assessed by a Mann–Whitney test (significance for $P<0.05$). With regard to the mean subjective image quality of all arterial segments combined, the differences between both types of MRA were assessed with a Wilcoxon signed rank test ($P<0.05$) in a per-patient analysis. In a per-arterial segment subanalysis, the differences between the two types of MRA with regard to the subjective image quality of each of the eight different arterial segments were evaluated with a paired sign test (significance $P<0.0063$ after Bonferroni correction). For these analyses the proportion-procedure for survey data of the Stata software (StataCorp, College Station, Texas) with the patient as primary sample unit was performed to address dependencies between segments.

Inter-observer agreement between the two readers (readers 1 and 2) and agreement between the two types of MRA for grading arterial stenosis were determined by calculating κ values (poor agreement, κ=0; slight agreement, κ=0.01–0.20; fair agreement, κ=0.21–0.40; moderate agreement, κ=0.41–0.60; good agreement, κ=0.61–0.80; and excellent agreement, κ=0.81–1.00) [25]. Because of dependencies between segments, confidence intervals for kappa values were not calculated.

Sensitivity, specificity, positive and negative predictive values, and accuracy including 95% CIs of the two types of MRA for detection of haemodynamically significant arterial stenosis compared with MDCTA were calculated for all arterial segments combined. To address dependencies of image analysis within the same patient, 95% CIs were calculated by using the proportion-procedure for survey data of the Stata software with the patient as the primary sample unit. The statistical significance of the differences in sensitivities between the two types of MRA for both readers was assessed by analysing true findings per patient using the paired sign test (significance $P<0.025$ after Bonferroni correction).

Results

Quantitative MR image analysis

SNR and CNR were measured for the abdominal aorta and the visceral arteries on both types of MRA in all 18 patients (Table 1). A total of 141/144 arterial segments could be assessed for fast MRA (98%; all arterial segments with moderate or better visibility as rated by both readers, see

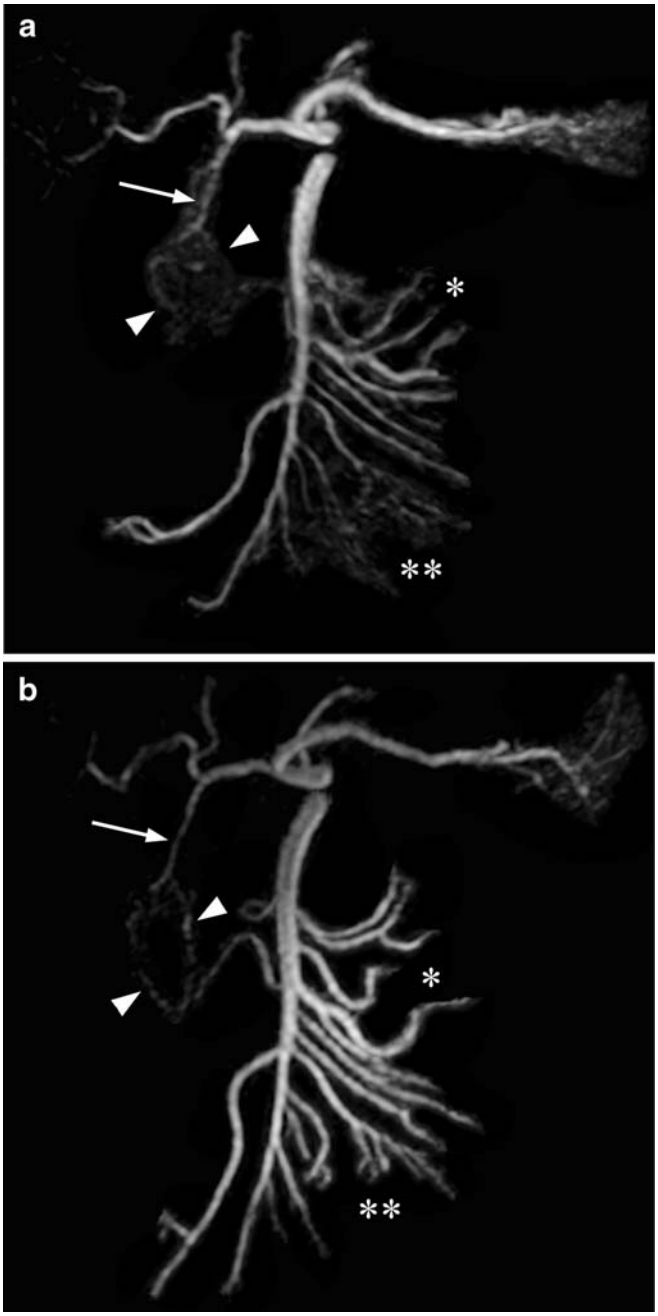

Fig. 2 Frontal maximum intensity projections of the celiac trunk and the superior mesenteric artery (SMA) and their branches reconstructed from coronal 3D contrast-enhanced **a** conventional (3.5/0.9) and **b** fast (4.2/1.3) MRA data sets in a 27-year-old man. The gastroduodenal artery (*arrow*) and the pancreaticoduodenal arcades (*arrowheads*) as well as the jejunal (*asterisk*) and ileal arteries (*double asterisk*) can be better delineated on fast compared with conventional MRA because of reduced motion-related artefacts, although signal-to-noise and contrast-to-noise ratios are higher on conventional MRA. Note, abdominal aorta and renal arteries were subtracted for better visualisation of the visceral artery anatomy

below) and 138/144 arterial segments for conventional MRA (96%). SNR (P=0.001) and CNR (P=0.001) were significantly higher on conventional than on fast MRA (Fig. 2).

Qualitative MR image analysis

Grading of subjective image quality of the abdominal aorta and the visceral arteries on both types of MRA were rated independently by both readers. There was a trend towards a better mean subjective image quality of all eight arterial segments on fast compared with conventional MRA. Both readers noted fewer motion-induced artefacts on fast MRA than on conventional MRA (Fig. 2). A total of 1% of all visceral segments were non-diagnostic on fast MRA (2% for reader 1 and 0% for reader 2), compared with 4% on conventional MRA. However, increased overall image quality on fast MRA compared with conventional MRA was statistically significant only for reader 2 (P=0.012) and not for reader 1 (P=0.055).

In the subanalysis of each of the eight arterial segments (Table 2, subanalysis for single segments with significance level set at P<0.0063 after Bonferroni correction), there was a trend towards better image quality on fast MRA compared with conventional MRA for both readers (Fig. 3). However, no statistically significant difference between the two techniques could be found for either reader. The trend towards better image quality on fast MRA for reader 2 was most pronounced for the celiac artery (P=0.06), the common hepatic artery (P=0.07) and the superior mesenteric artery (P=0.06), whereas for reader 1 the trend towards better image quality on fast MRA was not distinct for specific vessel segments (range of P=0.39–0.63 for all segments).

Stenosis of visceral arteries

For all grades of arterial stenosis, there was good inter-observer agreement for both conventional MRA (κ=0.68) and fast MRA (κ=0.80). For diagnosis of haemodynamically significant (grades 3 and 4) versus non-significant (grades 1 and 2) arterial stenoses, there was good inter-observer agreement for conventional (κ=0.76) and excellent inter-observer agreement for fast MRA (κ=1.00).

True-positive, true-negative, false-positive and false-negative findings, as well as sensitivities, specificities, positive and negative predictive values, and accuracies for diagnosing haemodynamically significant arterial stenosis of the analysed segments were calculated (Table 3). On fast MRA, both reader 1 and reader 2 correctly identified all 9 haemodynamically significant stenoses (Fig. 4) and all 132 segments without haemodynamically significant stenoses (sensitivity and specificity, 100% respectively, for both readers on fast MRA). Sensitivity of conventional MRA was 89% for both readers, and specificity was 100% for reader 1 and 99% for reader 2. However, differences in sensitivity between the two types of MRA were not statistically significant for either reader (P=0.25).

Table 2 Image quality of the abdominal aorta and visceral arteries as assessed by two independent readers on conventional and fast magnetic resonance angiography images in 18 patients

	Image quality of artery											Image quality of artery										
	Reader 1											Reader 2										
	Conventional MRA					Fast MRA						Conventional MRA					Fast MRA					
	1	2	3	4	5	1	2	3	4	5	*P*-value	1	2	3	4	5	1	2	3	4	5	*P*-value
Suprarenal aorta	0	0	0	2	16	0	0	0	0	18	0.5	0	0	0	1	17	0	0	0	0	18	0.5
Infrarenal aorta	0	0	0	4	14	0	0	0	4	14	0.5	0	0	0	3	15	0	0	0	2	16	0.5
Celiac trunk	0	0	2	5	11	0	0	0	6	12	0.45	0	0	2	8	8	0	0	1	5	12	0.06
Left gastric artery	1	1	4	6	6	0	0	5	6	7	0.51	0	2	2	9	5	0	1	3	9	5	1
Splenic artery	0	2	2	12	2	0	0	2	9	7	0.39	0	2	1	10	5	0	1	2	6	9	0.13
Common hepatic artery	0	2	1	7	8	0	0	2	7	9	0.55	0	2	1	11	4	0	1	1	7	9	0.07
Superior mesenteric artery	0	0	2	6	10	0	0	1	6	11	0.63	0	0	2	8	8	0	0	2	3	13	0.06
Inferior mesenteric artery	0	0	2	6	10	0	0	0	7	11	0.63	0	0	3	5	10	0	0	0	7	11	0.5
Total	1	5	13	48	77	0	0	10	45	89	0.055	0	6	11	55	72	0	3	9	39	93	0.012

Grade 1 Not visible (no diagnostic information can be obtained from the images), *2* poor visibility (image quality of the vessel is degraded because of low signal intensity *and* motion-induced blurring artefacts), *3* moderate visibility (image quality of the vessel is degraded because of low signal intensity *or* motion-induced blurring artefacts), *4* good visibility (high signal intensity *and* slight motion-induced blurring artefacts), *5* excellent visibility (high signal intensity, no motion-induced blurring artefacts). *MRA* Magnetic resonance angiography
Subanalysis for single segments with significance level set at P<0.0063 after Bonferroni correction

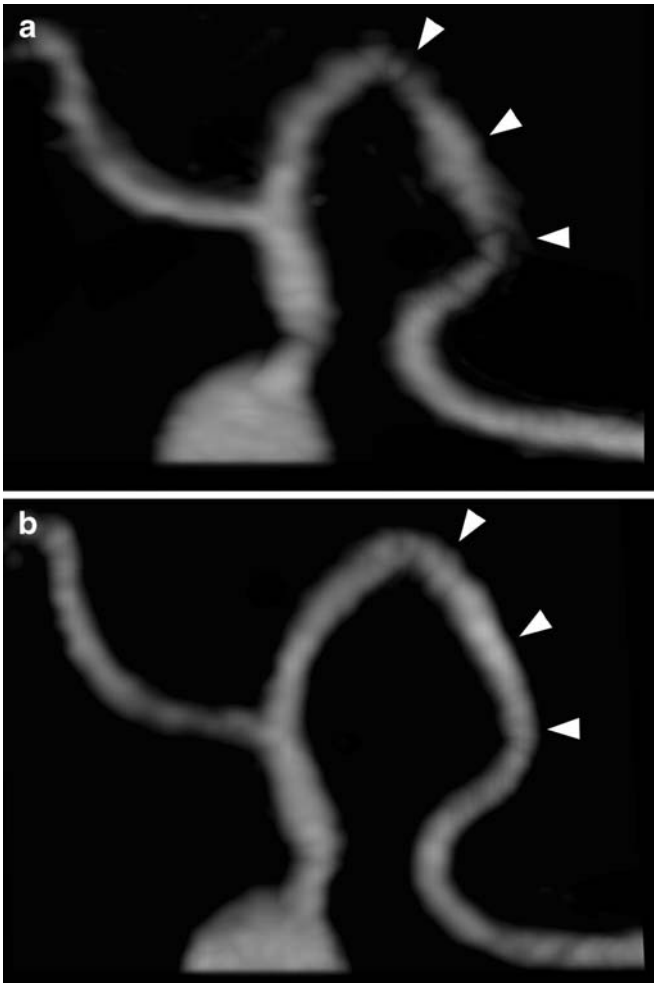

Fig. 3 Focused transverse maximum intensity projections of the celiac trunk branching into the common hepatic artery and the splenic artery of **a** conventional (3.5/0.9) and **b** fast (4.2/1.3) MRA data sets in a 73-year-old woman. Because of motion-induced artefacts, both readers rated the image quality of the splenic artery (*arrowheads*) as poor (grade 2) on conventional MRA and as excellent (grade 5) on fast MRA

Discussion

In our study, overall subjective image quality for depiction of visceral arteries was rated better on fast MRA than on conventional MRA. Both readers noted that image quality on fast MRA improved primarily because of reduced motion-related blurring artefacts compared with conventional MRA. Motion of the proximal branches of the abdominal aorta is a well-known limitation when imaging visceral arteries on MRA [7, 8]. In a recent investigation of image quality of conventional MRA in assessing visceral arteries, the authors pointed out that image quality of celiac, mesenteric and hepatic arteries was impaired because of motion-induced blurring artefacts in the subgroup of patients not able to hold their breath for the entire duration of image acquisition [7]. This phenomenon has been known since the early studies on abdominal MRA [9] and affected as many as 16% of patients undergoing conventional MRA in a recent study [7].

Blurring artefacts in proximal visceral arteries are caused by small movements of the diaphragm during breath-holding [26], by motion triggered through cardiac contraction and pulsatile oscillations of the aorta and its branches [27, 28], as well as by motion as a result of intestinal peristalsis [29]. Motion-induced artefacts during breath-holding are also reported for renal arteries [30], and fast MRA has been shown in a recent study to improve image quality of the distal segments of the renal arteries in particular [17]. We found similar effects regarding image quality of visceral arteries when using fast MRA compared with conventional MRA in our study. Reader 1 rated 93% of vessels as good or excellent on fast MRA and 86% on conventional MRA. For reader 2, the differences in image quality were most pronounced for the celiac trunk, the common hepatic artery and the superior mesenteric artery, with 92% of all vessels rated as good or excellent on fast MRA and 88% on conventional MRA. For reader 2 the overall image quality between the two types of MRA showed a statistically significant difference, whereas for reader 1 there was a trend towards better image quality for

Table 3 Performance of conventional and fast magnetic resonance angiography as assessed by two independent readers compared with 64-detector-row computed tomography in the detection of haemodynamically significant stenosis of visceral arteries in 18 patients

		All segments	
		Conventional MRA	Fast MRA
True positive	Reader 1	8	9
	Reader 2	8	9
True negative	Reader 1	132	132
	Reader 2	130	132
False positive	Reader 1	0	0
	Reader 2	2	0
False negative	Reader 1	1	0
	Reader 2	1	0
Sensitivity	Reader 1	89 (82, 96)	100 (100, 100)
	Reader 2	89 (82, 96)	100 (100, 100)
Specificity	Reader 1	100 (100, 100)	100 (100, 100)
	Reader 2	99 (98, 99)	100 (100, 100)
PPV	Reader 1	100 (100, 100)	100 (100, 100)
	Reader 2	80 (72, 88)	100 (100, 100)
NPV	Reader 1	99 (99, 99)	100 (100, 100)
	Reader 2	99 (99, 99)	100 (100, 100)
Accuracy	Reader 1	99 (99, 99)	100 (100, 100)
	Reader 2	98 (98, 98)	100 (100, 100)

Numbers *in parentheses* are 95% confidence interval
PPV Positive predictive value, *NPV* negative predictive value, *MRA* magnetic resonance angiography

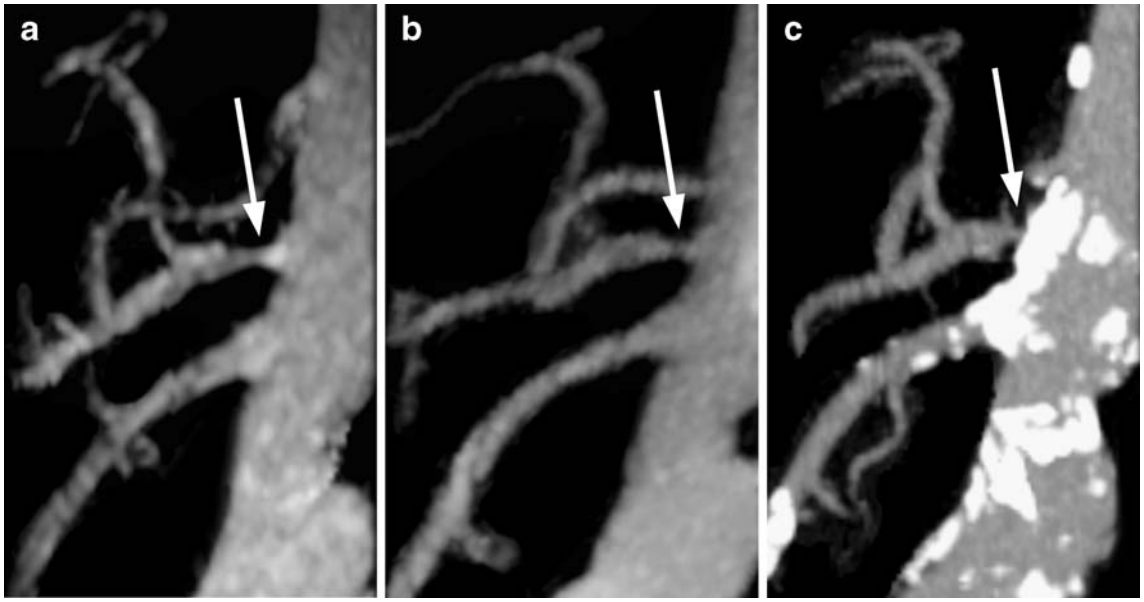

Fig. 4 Oblique sagittal maximum intensity projections of the abdominal aorta and its proximal branches reconstructed from coronal 3D contrast-enhanced **a** conventional (3.5/0.9) and **b** fast (4.2/1.3) MRA data sets in a 77-year-old man. Both readers rated celiac trunk stenosis (*arrow*) as haemodynamically significant (grade 3), which was confirmed on sagittal maximum intensity projection reconstruction of the MDCTA data set (**c**)

fast MRA. The inferior mesenteric artery, although less prone to respiration-induced blurring artefacts, was also better visualised on fast than on conventional MRA for both readers.

The higher image quality of fast MRA in our study is reflected in the higher sensitivity and specificity values for the detection of arterial stenosis. This finding is in line with a recent report on parallel acquisition MRA at 3.0 T with a sensitivity of 100% and a specificity of 94% compared with digital subtraction angiography in detecting visceral arterial stenosis [31]. In our study, all stenoses depicted on MDCTA were correctly classified on fast MRA by both readers. Consequently, inter-observer agreement for the detection of arterial stenosis was excellent for fast MRA. Despite a trend towards better results for fast MRA in the depiction of arterial stenosis, differences in sensitivity and specificity between the two types of MRA were not statistically significant.

Recently, MRA imaging protocols have become available for 3.0-T MR systems. Implementing parallel imaging at 3.0 T provides an additional improvement in image quality of contrast-enhanced MRA of visceral arteries, since at 3.0 T the MRA can be performed with a higher spatial resolution and a faster image acquisition [16, 32] and the higher CNR at 3.0 T can be used to further reduce the administered dose of MR contrast agent [32, 33]. A recent study has shown better visibility of visceral arteries on MR angiograms acquired on a 3.0-T MR system versus a 1.5-T system in 14 of 15 volunteers [34], and another group obtained reliable high-spatial-resolution images of the abdominal arteries with a parallel acquisition at 3.0 T in 32 patients with excellent sensitivity and specificity values for detection of haemodynamically significant arterial stenosis [31]. However, 3.0-T MRA approaches involve several technical challenges, including the need for a homogeneous radio frequency field that is more demanding to produce at 3.0 T than at 1.5 T, and a four-fold increased specific absorption rate compared to 1.5-T scanners [35].

Fast MRA may be of value in patients unable to undergo MDCTA because of known contraindications such as allergic reactions to iodine contrast or relative contraindications such as young age. In particular for patients unable to hold their breath, fast MRA may be advantageous over conventional MRA for the assessment of the aorta and visceral arteries. In addition, the fast MRA protocol described in our study allows assessment of the vasculature of the entire abdomen and pelvis including the iliac arteries. This may be advantageous in patients with general atherosclerosis and the need for an assessment of both the abdominal and pelvic vasculature in one imaging session.

We acknowledge several limitations of this retrospective study. As we did not compare patients both with and without restricted respiratory function, the true differences in image quality, sensitivity and specificity achieved by a reduction in acquisition time in patients with breath-holding difficulties cannot be directly estimated from the results of our study. Furthermore, our retrospective analysis only yielded 18 patients undergoing both fast and conventional MRA as well as MDCTA as a reference standard within a 60-day time interval. In addition, the limited prevalence of haemodynamically significant arte-

rial stenosis affecting 9 of the 141 segments (6%) restricts the calculated descriptive statistics in our study. Additional prospective studies with larger numbers of patients are warranted to confirm our results. Finally, as MDCTA was used as the reference standard, the actual extent of stenosis in segments that are heavily calcified may have been overrated on MDCTA, and therefore MDCTA was not an ideal reference standard in our study.

In conclusion, the results of our study suggest that fast and conventional MRA of the visceral arteries do not differ substantially in image quality or in the detection of arterial stenosis, despite a reduction in signal-to-noise and contrast-to-noise ratios on fast compared with conventional MRA. Therefore, in patients unable to hold their breath, fast MRA may be a valuable alternative to conventional MRA for the assessment of visceral arteries.

References

1. Cognet F, Ben Salem D, Dranssart M et al (2002) Chronic mesenteric ischemia: imaging and percutaneous treatment. Radiographics 22:863–879
2. Horton KM, Fishman EK (2007) Multidetector CT angiography in the diagnosis of mesenteric ischemia. Radiol Clin North Am 45:275–288
3. Shih M-CP, Hagspiel KD (2007) CTA and MRA in mesenteric ischemia: part 1, role in diagnosis and differential diagnosis. AJR Am J Roentgenol 188:452–461
4. Meaney JF, Prince MR, Nostrant TT, Stanley JC (1997) Gadolinium-enhanced MR angiography of visceral arteries in patients with suspected chronic mesenteric ischemia. J Magn Reson Imaging 7:171–176
5. Hany TF, Schmidt M, Schoenenberger AW, Debatin JF (1998) Contrast-enhanced three-dimensional magnetic resonance angiography of the splanchnic vasculature before and after caloric stimulation. Original investigation. Invest Radiol 33:682–686
6. Heiss SG, Li KC (1998) Magnetic resonance angiography of mesenteric arteries. A review. Invest Radiol 33:670–681
7. Billaud Y, Beuf O, Desjeux G, Valette PJ, Pilleul F (2005) 3D contrast-enhanced MR angiography of the abdominal aorta and its distal branches: interobserver agreement of radiologists in a routine examination. Acad Radiol 12:155–163
8. Ernst O, Asnar V, Sergent G et al (2000) Comparing contrast-enhanced breath-hold MR angiography and conventional angiography in the evaluation of mesenteric circulation. AJR Am J Roentgenol 174:433–439
9. Prince MR, Narasimham DL, Stanley JC et al (1995) Breath-hold gadolinium-enhanced MR angiography of the abdominal aorta and its major branches. Radiology 197:785–792
10. Sodickson DK, Manning WJ (1997) Simultaneous acquisition of spatial harmonics (SMASH): fast imaging with radiofrequency coil arrays. Magn Reson Med 38:591–603
11. Pruessmann KP, Weiger M, Scheidegger MB, Boesiger P (1999) SENSE: sensitivity encoding for fast MRI. Magn Reson Med 42:952–962
12. Heilmaier C, Sutter R, Lutz AM et al (2007) Mapping of hepatic vascular anatomy: dynamic contrast-enhanced parallel MR imaging compared with 64 detector row CT. Radiology 245:872–880
13. McKenzie CA, Lim D, Ransil BJ et al (2004) Shortening MR image acquisition time for volumetric interpolated breath-hold examination with a recently developed parallel imaging reconstruction technique: clinical feasibility. Radiology 230:589–594
14. Werder R, Nanz D, Lutz AM et al (2007) Assessment of the abdominal aorta and its visceral branches by contrast-enhanced dynamic volumetric hepatic parallel magnetic resonance imaging: feasibility, reliability and accuracy. Eur Radiol 17:541–551
15. Xu PJ, Yan FH, Wang JH, Lin J, Fan J (2007) Utilizing generalized autocalibrating partial parallel acquisition (GRAPPA) to achieve high-resolution contrast-enhanced MR angiography of hepatic artery: initial experience in orthotopic liver transplantation candidates. Eur J Radiol 61:507–512
16. Ho LM, Merkle EM, Paulson EK, Dale BM (2007) Contrast-enhanced hepatic magnetic resonance angiography at 3 T: does parallel imaging improve image quality? J Comput Assist Tomogr 31:177–180
17. Sutter R, Nanz D, Lutz AM et al (2007) Assessment of aortoiliac and renal arteries: MR angiography with parallel acquisition versus conventional MR angiography and digital subtraction angiography. Radiology 245: 276–284
18. Kroencke TJ, Wasser MN, Pattynama PM et al (2002) Gadobenate dimeglumine-enhanced MR angiography of the abdominal aorta and renal arteries. AJR Am J Roentgenol 179:1573–1582
19. Schoenberg SO, Bock M, Knopp MV et al (1999) Renal arteries: optimization of three-dimensional gadolinium-enhanced MR angiography with bolus-timing-independent fast multiphase acquisition in a single breath hold. Radiology 211:667–679
20. Goyen M, Herborn CU, Kroger K, Lauenstein TC, Debatin JF, Ruehm SG (2003) Detection of atherosclerosis: systemic imaging for systemic disease with whole-body three-dimensional MR angiography - initial experience. Radiology 227:277–282
21. Goldfarb JW (2004) The SENSE ghost: field-of-view restrictions for SENSE imaging. J Magn Reson Imaging 20:1046–1051
22. Goshima S, Kanematsu M, Kondo H et al (2006) MDCT of the liver and hypervascular hepatocellular carcinomas: optimizing scan delays for bolus-tracking techniques of hepatic arterial and portal venous phases. AJR Am J Roentgenol 187:W25–W32
23. Chen Q, Quijano CV, Mai VM et al (2004) On improving temporal and spatial resolution of 3D contrast-enhanced body MR angiography with parallel imaging. Radiology 231:893–899
24. Zenge MO, Vogt FM, Brauck K et al (2006) High-resolution continuously acquired peripheral MR angiography featuring partial parallel imaging GRAPPA. Magn Reson Med 56:859–865
25. Landis JR, Koch GG (1977) An application of hierarchical kappa-type statistics in the assessment of majority agreement among multiple observers. Biometrics 33:363–374

26. Shirkhoda A, Konez O, Shetty AN, Bis KG, Ellwood RA, Kirsch MJ (1998) Contrast-enhanced MR angiography of the mesenteric circulation: a pictorial essay. Radiographics 18:851–861 discussion 862–855
27. Jeays AD, Lawford PV, Gillott R et al (2007) Characterisation of the haemodynamics of the superior mesenteric artery. J Biomech 40:1916–1926
28. Wasser MN, Geelkerken RH, Kouwenhoven M et al (1996) Systolically gated 3D phase contrast MRA of mesenteric arteries in suspected mesenteric ischemia. J Comput Assist Tomogr 20:262–268
29. Schoepf UJ, Becker C, Bruning R et al (1999) Computed tomography of the abdomen with multidetector-array CT. Radiologe 39:652–661
30. Vasbinder GB, Maki JH, Nijenhuis RJ et al (2002) Motion of the distal renal artery during three-dimensional contrast-enhanced breath-hold MRA. J Magn Reson Imaging 16:685–696
31. Nael K, Saleh R, Lee M et al (2006) High-spatial-resolution contrast-enhanced MR angiography of abdominal arteries with parallel acquisition at 3.0 T: initial experience in 32 patients. AJR Am J Roentgenol 187: W77–W85
32. Chang KJ, Kamel IR, Macura KJ, Bluemke DA (2008) 3.0-T MR imaging of the abdomen: comparison with 1.5 T. Radiographics 28:1983–1998
33. Krautmacher C, Willinek WA, Tschampa HJ et al (2005) Brain tumors: full- and half-dose contrast-enhanced MR imaging at 3.0 T compared with 1.5 T–initial experience. Radiology 237:1014–1019
34. Michaely HJ, Kramer H, Dietrich O et al (2007) Intraindividual comparison of high-spatial-resolution abdominal MR angiography at 1.5 T and 3.0 T: initial experience. Radiology 244:907–913
35. Nael K, Laub G, Finn JP (2005) Three-dimensional contrast-enhanced MR angiography of the thoraco-abdominal vessels. Magn Reson Imaging Clin N Am 13:359–380